Exp Brain Res (1993) 97:13–22

Experimental Brain Research

Increased proportion of acetylcholinesterase-rich zones and improved morphological integration in host striatum of fetal grafts derived from the lateral but not the medial ganglionic eminence

P. Pakzaban[1, 2], **T.W. Deacon**[1], **L.H. Burns**[1], **O. Isacson**[1, 2]

[1]Neuroregeneration Laboratory, McLean Hospital, MRC 119, Belmont, MA 02178–9106, USA
[2]Departments of Neurosurgery and Neurology and Program in Neuroscience, Harvard Medical School, Massachusetts General Hospital, Boston, MA 02114, USA

Received: 5 April 1993 / Accepted: 21 June 1993

Abstract. Fetal striatal grafts are found to have a modular organization revealed by acetylcholinesterase (AChE) histochemistry. The AChE-rich zones represent the only portions of these grafts that are anatomically and functionally integrated into the host brain. In this study, the medial and lateral ganglionic eminences (MGEs and LGEs) were selectively dissected from the basal telencephalon of embryonic-day-14 (E14) rat fetuses to compare their relative contributions to the AChE-rich fraction of intrastriatal grafts. Separate cell suspensions prepared from either eminence were stereotaxically implanted into excitotoxically lesioned neostriatum of adult rats. Eight weeks after transplantation, grafts of the MGE were compared with those of the LGE with respect to the proportion of AChE-rich zones, graft size, graft morphology, and afferent dopaminergic innervation as revealed by tyrosine hydroxylase (TH) immunostaining. The mean AChE-rich fraction in LGE grafts (87% ± 4%) was markedly greater than the AChE-rich fraction in MGE grafts (25% ± 10%). The LGE grafts were also morphologically better incorporated into the lesioned host striatum, partially reconstituting the striatal morphology. There was no statistically significant difference in graft size between the two groups. The AChE-rich LGE grafts were TH immunoreactive, whereas the AChE-poor MGE grafts were not. We conclude that grafts derived exclusively from the fetal LGE reconstitute the striatal morphology and consist almost entirely of AChE-rich zones.

Key words: Neural transplantation – Fetal grafts – Huntington disease – Neural regeneration – Neural development – Rat

Introduction

Homotopic transplantation of fetal striatal primordium into excitotoxically lesioned neostriatum of adult rats provides a paradigm for the study of regenerative mechanisms in neural transplants and an animal model for the study of transplantation therapy in Huntington disease (Deckel et al. 1983, 1986; Dunnett et al. 1988; Hantraye et al. 1992; Helmes et al. 1992; Isacson et al. 1984, 1986; Wictorin and Björklund 1989; Wictorin et al. 1988, 1989a,b,c, 1990a,b, 1991). In these preparations, the striatal anlage that is usually dissected from the fetal telencephalon consists of both medial and lateral ganglionic eminences (MGE and LGE; Dunnett and Björklund 1992). Intrastriatal implantation of cells from these ganglionic eminences yields grafts which have a heterogeneous structure, readily recognizable by acetylcholinesterase (AChE) histochemistry (Graybiel et al. 1989; Isacson et al. 1987; Walker et al. 1987; Wictorin et al. 1989b). AChE-rich zones, which closely correspond to zones immunoreactive for dopamine and cyclic AMP-regulated phosphoprotein (DARPP-32), met-enkaphlin, substance P, tyrosine hydroxylase (TH), and choline acetyl transferase (ChAT), are interspersed amongst AChE-poor zones, which lack immunoreactivity for these striatal markers (Graybiel et al. 1989; Isacson et al. 1987; Wictorin et al. 1989b). Extensive evidence shows that only the AChE-rich zones of the graft are structurally and functionally integrated with the host brain circuitry (Campbell et al. 1992; Graybiel et al. 1989; Labandeira-Garcia et al. 1991; Liu et al. 1990, 1991; Mandel et al. 1992; Wictorin et al. 1988, 1989b,c). Graybiel et al. (1989) named these AChE-rich areas "P zones," to distinguish them from the remaining AChE-poor "NP zones".

Inasmuch as the AChE-rich zones represent striatal-like portions of the graft that are anatomically and functionally connected to the host, it may be desirable to increase the proportion of these zones within the graft. To accomplish this, a better understanding of the nature and origin of AChE-poor zones in striatal grafts is required. It has been suggested that AChE-poor zones may either represent non-striatal tissue contaminating the fetal striatal preparation or reflect aberrant development of some graft regions (Difiglia et al. 1988; Graybiel et al. 1989; Isacson et al. 1987). Specifically, regions of neuropil have

Correspondence to: P. Pakzaban

been identified within striatal grafts that have a synaptic and neuronal morphology reminiscent of globus pallidus (Difiglia et al. 1988). Furthermore, it has been argued that the ventral part of the MGE, which is coextensive with the pallidal anlage, may be a source for cells of the globus pallidus (Smart and Sturrock 1979; Marchand and Lajoie 1986; Nieuwenhuys 1977). Therefore, inclusion of the entire MGE within the limits of the dissection may be one source of nonneostriatal tissue within the graft.

In this study, we examined whether exclusion of putative nonneostriatal precursors from the grafts by highly selective dissection of the LGE would increase the proportion of AChE-rich zones within the grafts. Cell suspensions prepared from selectively dissected MGEs or LGEs were implanted into neuron-depleted striata, and the surviving grafts in the two groups were compared with respect to the proportion of AChE-rich zones, graft size, graft morphology, and afferent connectivity as revealed by TH immunostaining.

Materials and methods

Experimental design

Twenty adult male Sprague-Dawley rats (Charles River Laboratories, USA), weighing 300–350 g, received unilateral injections of quinolinic acid into the right neostriatum. Seven days later, ten lesioned animals received intrastriatal injections of a cell suspension prepared from the MGE of embryonic-day-14 (E14) fetal rat brains, while the other ten were transplanted with cells from the LGE of the same fetuses. After 8 weeks, the surviving animals (nine in each group) were killed, and the surviving grafts were characterized by Nissl stain (cresyl violet), AChE histochemistry, and TH immunohistochemistry.

Dissection of fetal telencephalic ganglionic eminences

The uterine horns were removed from two timed-mated, pregnant Sprague-Dawley rats on day 14 of pregnancy under pentobarbital terminal anesthesia. The E14 fetuses (crown-rump length 12–13 mm) were immediatedly delivered from their uterine pouches (12 fetuses per litter) and transferred to Dulbecco's phosphate-buffered saline (DPBS) with 1000 mg glucose /l (Sigma). The fetal brains were carefully extracted from the skull through a midsagittal incision and transferred individually to a sterile black ceramic saucer filled with DPBS (Fig. 1A). Dissection of the ganglionic eminences was perfomed under 40-fold magnification with the aid of a Zeiss OPMI-1 surgical microscope. The fetal brain was securely held with a pair of microforceps applied over the diencephalon, keeping the ventral forebrain surface against the saucer, in order to bring the dorsal surface of the cerebral hemispheres in sight (Fig. 1B). A parasagittal incision was created with straight microscissors (RS-5610; Roboz Surgical Instruments, Rockville, Md., USA) along the dorsal aspect of each hemisphere, exposing the MGE and LGE as they sit in the ventrolateral wall of the lateral ventricle (Fig. 1C,D). The dorsal incision was then circumferentially completed, coursing in the basal groove between the MGE and the diencephalon, thus detaching the ventrolateral wall of the hemisphere (carrying the ganglionic eminences) from the rest of the brain (Fig. 1D). The external (cortical) surface of the detached wall of the hemisphere was then flattened against the saucer, exposing the ganglionic eminences on the inner surface. In this position, the bulging medial eminence is clearly delimited from the more shallow and elongated lateral eminence by a fissure that is most prominent rostrally. Approaching from the rostral end, one blade of curved microscissors (RS-5611; Roboz) was then slipped into this fissure, while the other blade was placed on the medial surface of the medial eminence. The bulging head of the medial eminence was thus excised and transferred to a petri dish containing calcium- and magnesium-free Hank's balanced salt solution (HBSS; Sigma). The lateral eminence, now sitting as a single bulge overlying the cortex of the lateral wall of the hemisphere, was then readily excised along its base with curved microscissors held parallel to the cortex. The resected lateral eminence was transferred to a separate dish of HBSS. This dissection was performed on both hemispheres of all fetal brains, pooling the dissected tissue from the medial eminences separately from that of the lateral eminences.

Preparation of cell suspension

Preparation of the fetal cell suspensions was performed according to standard neuronal culture protocols (see Banker and Goslin 1991). The tissue fragments obtained from the dissection of the ganglionic eminences were incubated with 1 ml of 0.5% trypsin-EDTA in HBSS (Sigma) at 37° C for 10 min. The trypsin solution was then replaced with Iscov's modified Dulbecco's medium (IMDM) supplemented with 10% fetal bovine serum (FBS), penicillin (100 000 units/l), and streptomycin (100 mg/l; all from Sigma). The fragments were gently triturated through the tips of fire-polished Pasteur pipettes of progressively smaller internal diameter until a turbid suspension free of visible tissue fragments was obtained. Cell count and viability were determined by fluorescent microscopic examination of a 10–µl sample of the cell suspension diluted fivefold in a solution of acridine orange and ethidium bromide, as previously described (Brundin et al. 1985). The volumes were then adjusted to achieve the same viable cell concentration in both cell suspensions (see below).

Lesion and transplantation surgery

Animals were anesthetized by intraperitoneal injection of pentobarbital (65 mg/kg), and placed in a Kopf stereotaxic frame. A 5–µl Hamilton syringe attached to a 26S-gauge needle (ID/OD 0.11 mm/0.46 mm) was used to deliver 120 nmol (1 µl) of quinolinic acid into the right neostriatum of each animal (coordinates in relation to bregma: anterior +1.0, lateral −2.5, ventral −4.5 mm; incisor bar at −2.5 mm) over 1 min. The needle was withdrawn after an additional minute. Seven days later, the quinolinic acid-lesioned animals were anesthetized as before, in preparation for cell transplantation. Fetal ganglionic eminence cell suspensions were prepared as described above. A 10–µl Hamilton syringe attached to a 22S-gauge needle (ID/OD 0.41 mm/0.71 mm) was used to carefully deliver 5 µl of either the MGE or the LGE cell suspension (90 000 viable cells per microliter) to the right neostriatum at the same coordinates as used for the lesion. The cell suspension was injected as a single, slow bolus, administered over 10 min. The needle was slowly withdrawn after 2 min.

Perfusion and tissue processing

Eight weeks after cell transplantation, the animals were terminally anesthetized with an overdose of pentobarbital, in preparation for perfusion. The animals were perfused through the left ventricle with a heparin-saline solution (1000 units of heparin/–l 0.9% saline), followed by 300–400 ml of 4% paraformaldehyde in 100 mM phosphate buffer (pH 7.4). The brains were immediately removed and postfixed for 8 h in the same 4% paraformaldehyde solution, before immersion in 30% sucrose in phosphate-buffered saline (PBS; pH 7.4). Two days later, 50–µm sections through the striatum were cut on a freezing microtome and collected in PBS.

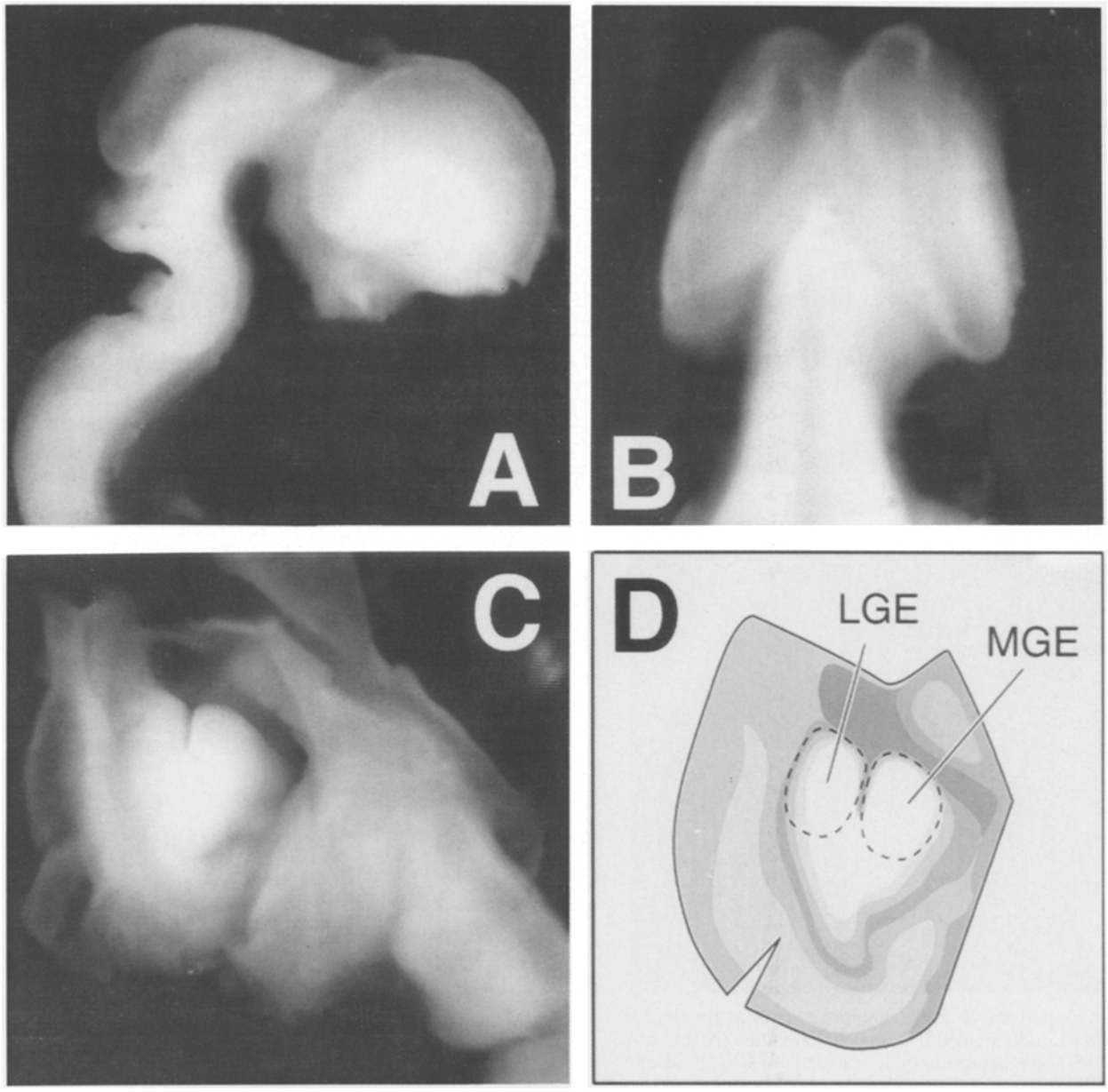

Fig. 1A–D. Three views of a fetal rat brain at age E14 showing the position and orientation of the fetal telencephalic ganglionic eminences and how they were dissected. **A** Right side. **B** Close-up of the two cerebral hemispheres as viewed from above. **C** Left cerebral hemisphere opened by cutting the overlying cortex to expose the floor and lateral wall of the lateral ventricle and the telencephalic ganglionic eminences. The view is from the top, as in **B**, with rostral toward the *top* and left toward the *left edge*. **D** The ganglionic eminences as in **C**. The *dashed lines* encircling the tip of each ganglionic eminence indicate the portions of each that were selectively dissected

AChE histochemistry was performed according to the method of Koelle (1954). Briefly, slide-mounted sections were incubated for 6 h in the incubation medium containing 30 mM sodium acetate buffer, pH 5.0, 9 mM copper sulphate, 16 mM glycine, 4 mM acetyl thiocholine iodide, and 0.1 mM ethopropazine. After the incubation, the slides were washed with distilled water, developed in 10% potassium ferricyanide, and washed again in distilled water prior to exposure to 0.5% sodium sulphide for 30–40 s. Adjacent sections were stained with cresyl violet.

For TH immunohistochemistry, every fourth section was preincubated in 10% normal goat serum in PBS for 1 h. The sections were then incubated overnight with primary antiserum, raised in rabbit against TH (East Acres Biologicals, USA), diluted 1:500 in 1% normal goat serum, 2% bovine serum albumin, and 0.1% Triton-X in PBS. Following 90–min incubations with goat anti-rabbit biotinylated secondary antibody at a 1:200 dilution in PBS and 1% normal goat serum, the sections were incubated with the avidin-biotin complex (Vector, USA) prior to the final reaction with 0.5% 3,3'-diaminobenzidine and 0.04% nickel chloride in 0.4% H_2O_2 and TBS for 1–2 min. The sections were washed with PBS after each incubation.

Morphometric analysis

The quantification of total graft volumes and component AChE-rich and -poor fractions of the grafts was performed with the aid of

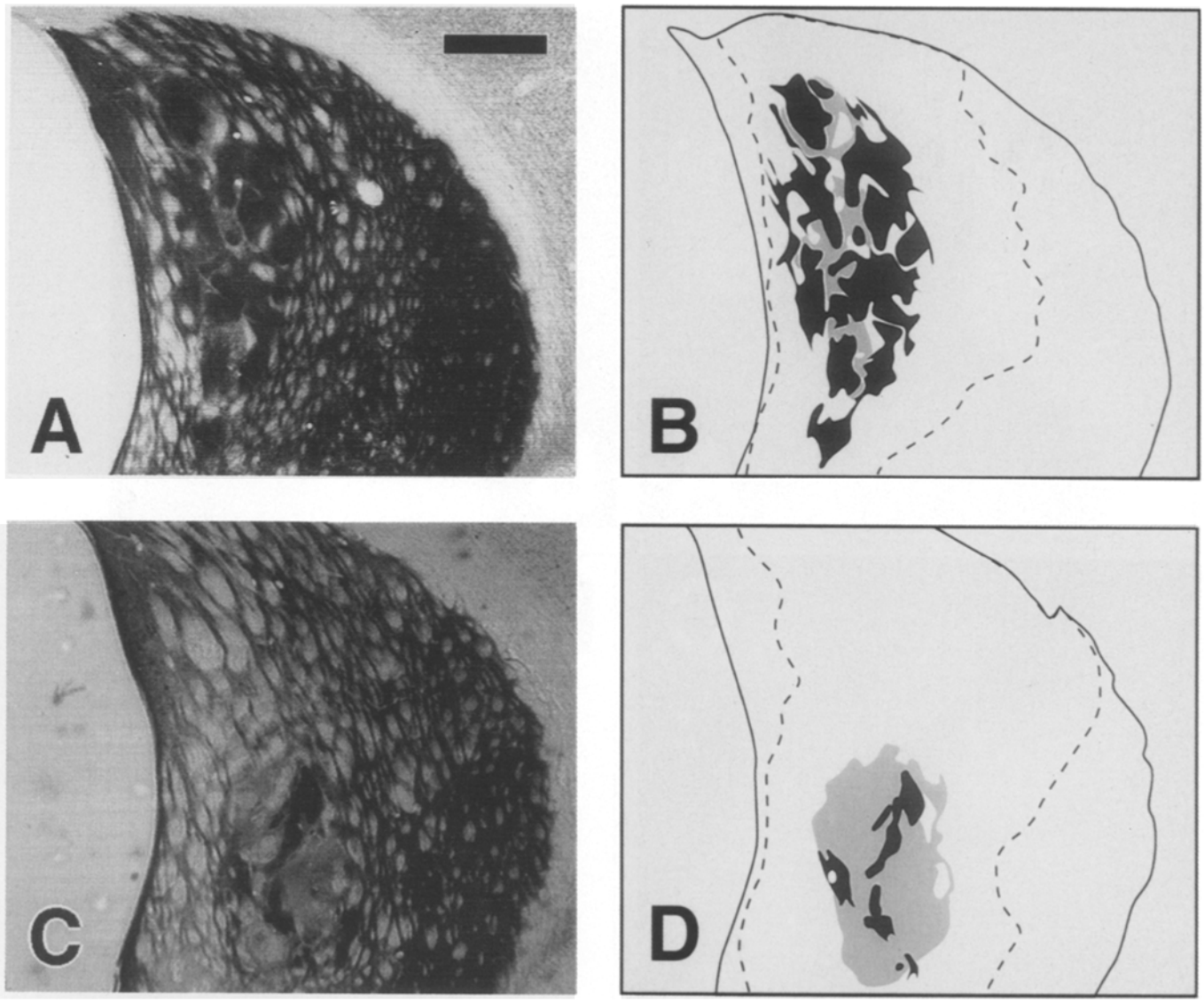

Fig. 2A–D. Comparison of two representative intrastriatal ganglionic eminence grafts stained by acetylcholinesterase (AChE) histochemistry with companion graphic tracings of each to indicate the distinction between AChE-rich and -poor zones within the grafts. **A,B** Lateral ganglionic eminence-derived graft; **C,D** medial ganglionic eminence-derived graft. In the tracings, AChE-rich zones are *dark-gray regions* and AChE-poor zones are *light gray regions.* The differences in proportions of AChE-rich and -poor zones in the two types of grafts are clearly evident. *Scale bar* 100 μm

computer image analysis (Image v.1.44 run on a Macintosh II computer equipped with a Mass Microsystems ColorSpace II video card) of a video image from a Zeiss Axioplan microscope. Images were contrast-enhanced to increase distinctions between differently stained tissues, but no computational manipulations of the images were performed. For quantification, microscope images were projected as live video on the computer screen, and AChE-rich and -poor zones were traced in a calibrated image analysis window that was directly superimposed on top of the video microscope image. Examples of typical tracings and matching microscope images are shown in Fig. 2. White matter tracts that penetrated the grafts in many cases (see below), as is typical of normal striatal architecture, were excluded from the quantification of cross-sectional areas and the total graft volume. The white matter tracts were often easily distinguishable from the AChE-poor zones within the graft based on their circumscribed geometry and complete absence of staining with AChE. In cases where the distinction between white matter and AChE-poor zones was ambiguous it could be readily resolved by examination of adjacent Nissl-stained sections. After automated quantification of AChE-rich and -poor areas on each section, the volume of each zone was calculated by integration of these cross-sectional areas over the length of the graft. Total graft volume was defined as the sum of volumes of AChE-rich and -poor zones (excluding white matter tracts). The AChE-rich fraction was calculated by dividing the volume of AChE-rich zones by the total graft volume.

Results

Cell viability and graft survival

The cell suspensions prepared from the LGEs and MGEs were found to have 86% and 82% viability, respectively,

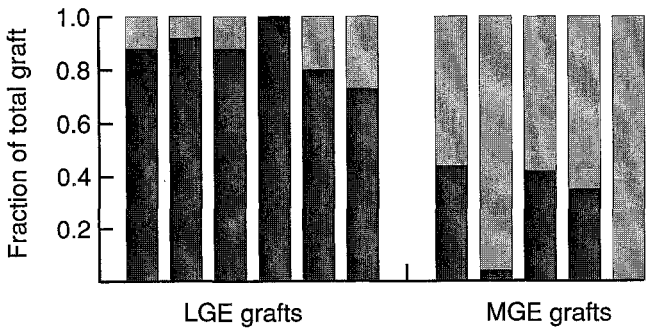

Fig. 3. The relative proportions of acetylcholinesterase- (AChE)-rich (*dark shading*) and -poor (*light shading*) zones in individual lateral (*LGE*) and medial (*MGE*) ganglionic eminence grafts. All proportions are represented as fractions of the entire graft (1.0) in each case, to control for differences in total graft size. One graft of each type was completely homogeneous, comprised exclusively of AChE-rich or AChE-poor zones

immediately prior to transplantation. Eight weeks after transplantation, six of the nine animals in the lateral group and five of the nine animals in the medial group were found to have viable grafts by AChE and Nissl staining. The average net volume (excluding white matter tracts incorporated in the graft) of the LGE grafts was $0.82 \pm 0.19\ mm^3$ (mean $\pm$ SEM), whereas that of the MGE grafts was $0.32 \pm 0.17\ mm^3$. Although there was a tendency toward smaller graft size in the MGE group, this difference was not statistically significant ($P = 0.09$, unpaired Student's t-test).

Comparison of AChE-rich fractions in LGE and MGE grafts

Figure 2A,C demonstrates sections through a typical LGE and a typical MGE graft, respectively. The corresponding tracings used for calculation of the AChE-rich and -poor fractions are presented in Fig. 2B,D. The higher proportion of AChE-rich zones in this LGE graft is readily apparent. The calculated AChE-rich and -poor fractions for each of the grafts in this study are presented in Fig. 3: the mean AChE-rich fraction in the LGE grafts was $0.87 \pm .04$, as compared to the mean AChE-rich fraction of 0.25 ± 0.1 in the MGE grafts. The difference between the two groups was highly significant ($P < 0.0001$, Student's t-test). As demonstrated in Fig. 3, the ranges of the AChE-rich fractions in the two groups were totally non-overlapping (0.73–1.00 in the LGE group vs 0–0.44 in the MGE group). Also note that one of the grafts in the LGE group was comprised exclusively of AChE-rich tissue (Fig. 4A), whereas one of the grafts in the MGE group consisted solely of AChE-poor tissue (Fig. 4B).

Graft morphology

Compared with the grafts derived from the MGE, those derived from the LGE were morphologically better incorporated into the lesioned host striatum. This morphological difference is well demonstrated in Fig. 4. The AChE-rich LGE graft (Fig. 4A) demonstrates an interstitial growth pattern, growing between the white matter tracts, but not pushing these tracts apart. In contrast, the AChE-poor MGE graft (Fig. 4B) exhibits a growth pattern in which expansion of the graft outwardly displaces the white matter tracts of the internal capsule. Nissl-stained adjacent sections (Fig. 4C,D) reveal both graft types to be highly cellular and clearly distinguishable from the surrounding neuron-depleted host striatum. Comparison of the Nissl-stained sections under higher magnification (Fig. 5A,B) reveals no obvious differences in cell size and morphology that would distinguish LGE grafts from MGE grafts.

TH immunohistochemistry

TH immunostaining on adjacent sections of selected grafts corresponded to the pattern of AChE staining. The purely AChE-rich LGE graft depicted in Fig. 4A,C,E showed significantly higher immunoreactivity for TH than the purely AChE-poor MGE graft shown in Fig. 4B,D,F. The portions of the striatum spared by the quinolinic acid lesion (e.g., the periventricular region in Fig. 4E,F) were highly TH immunoreactive and served as positive controls.

Discussion

We found that striatal grafts derived from the selectively dissected LGE of the fetal telencephalon have a significantly greater proportion of AChE-rich zones than those derived from the MGE. Furthermore, the AChE-rich grafts grow in the interstices between the fiber bundles that penetrate the striatum, thus reconstituting the normal striatal morphology. In contrast, AChE-poor grafts exclude these fiber bundles and displace them outward from the expanding graft, thereby distorting the morphology of the striatum. Finally, the AChE-rich grafts derived from the LGE become richly innervated by host afferent dopaminergic axons, as demonstrated by their TH immunoreactivity, whereas AChE-poor grafts derived from the MGE do not.

The significance of these observations is threefold. First, from a methodological standpoint, it is desirable to increase the AChE-rich fraction in striatal grafts, since this is the portion of the graft that is structurally and functionally connected to the host brain (Campbell et al. 1992; Graybiel et al. 1989; Labandeira-Garcia et al. 1991; Liu et al. 1990, 1991; Mandel et al. 1992; Wictorin et al. 1988, 1989b,c). Secondly, these findings help elucidate the nature and origin of AChE-poor zones (NP zones), an issue that has received much attention in the literature (Difiglia et al. 1988; Graybiel et al. 1989; Isacson et al. 1987). Finally, this study utilizes neural transplantation as a tool for the study of striatal development and the fate of the telencephalic ganglionic eminences.

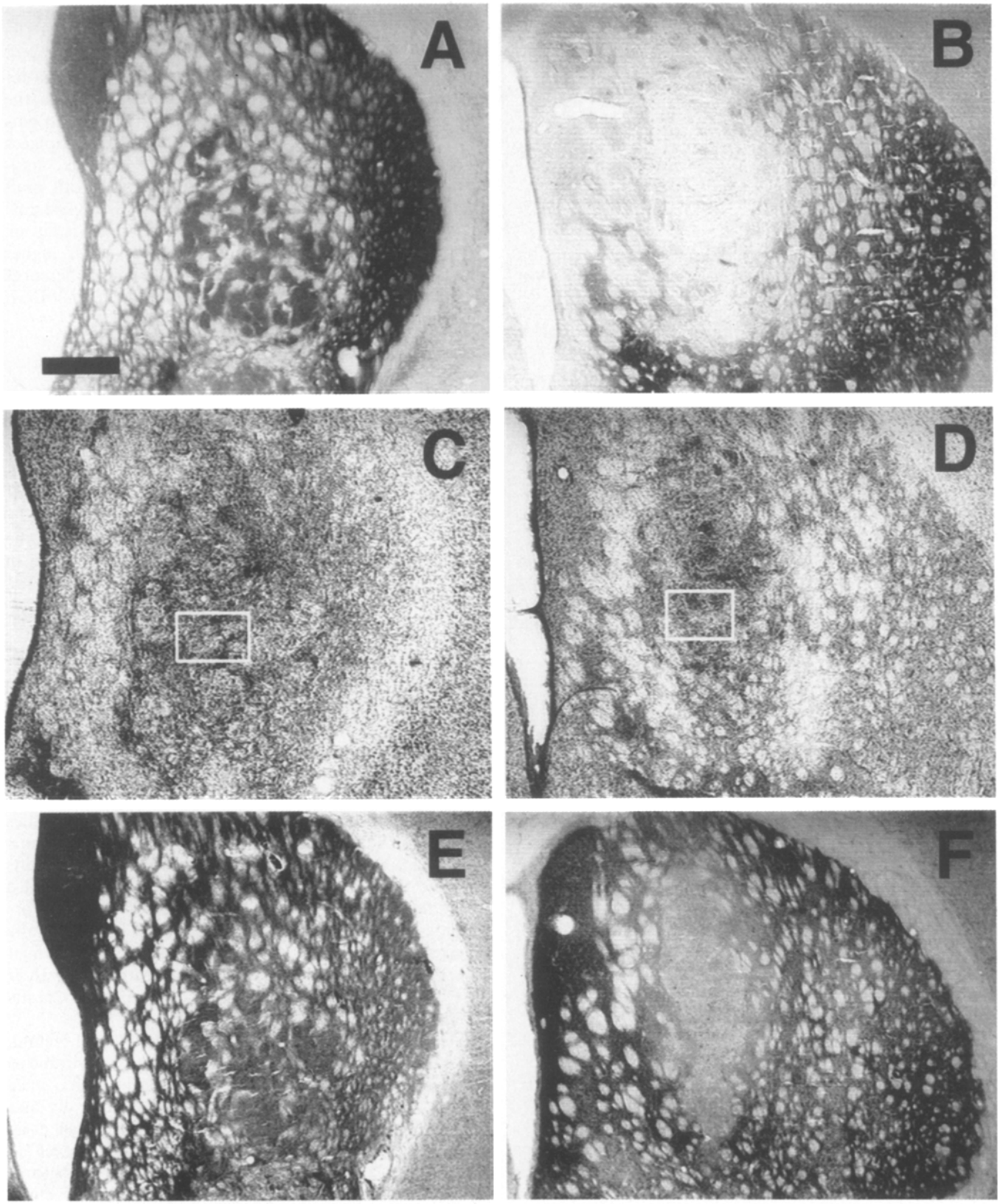

Fig. 4. Comparison of adjacent acetylcholinesterase- (AChE)-, Nissl, - and tyrosine hydroxylase- (TH)-stained sections of a completely AChE-rich lateral ganglionic eminence graft (**A,C,E**) and a completely AChE-poor medial ganglionic eminence graft (**B,D,F**). **A,B** AChE histochemical staining; **C,D** Nissl staining; **E,F** TH immunohistochemical staining. Despite the differences in AChE and TH staining, both grafts are equally cell dense (compare **C** and **D**). The *small white boxes* indicate the sites shown magnified in Fig. 5A,B. *Scale bar* 100 μm

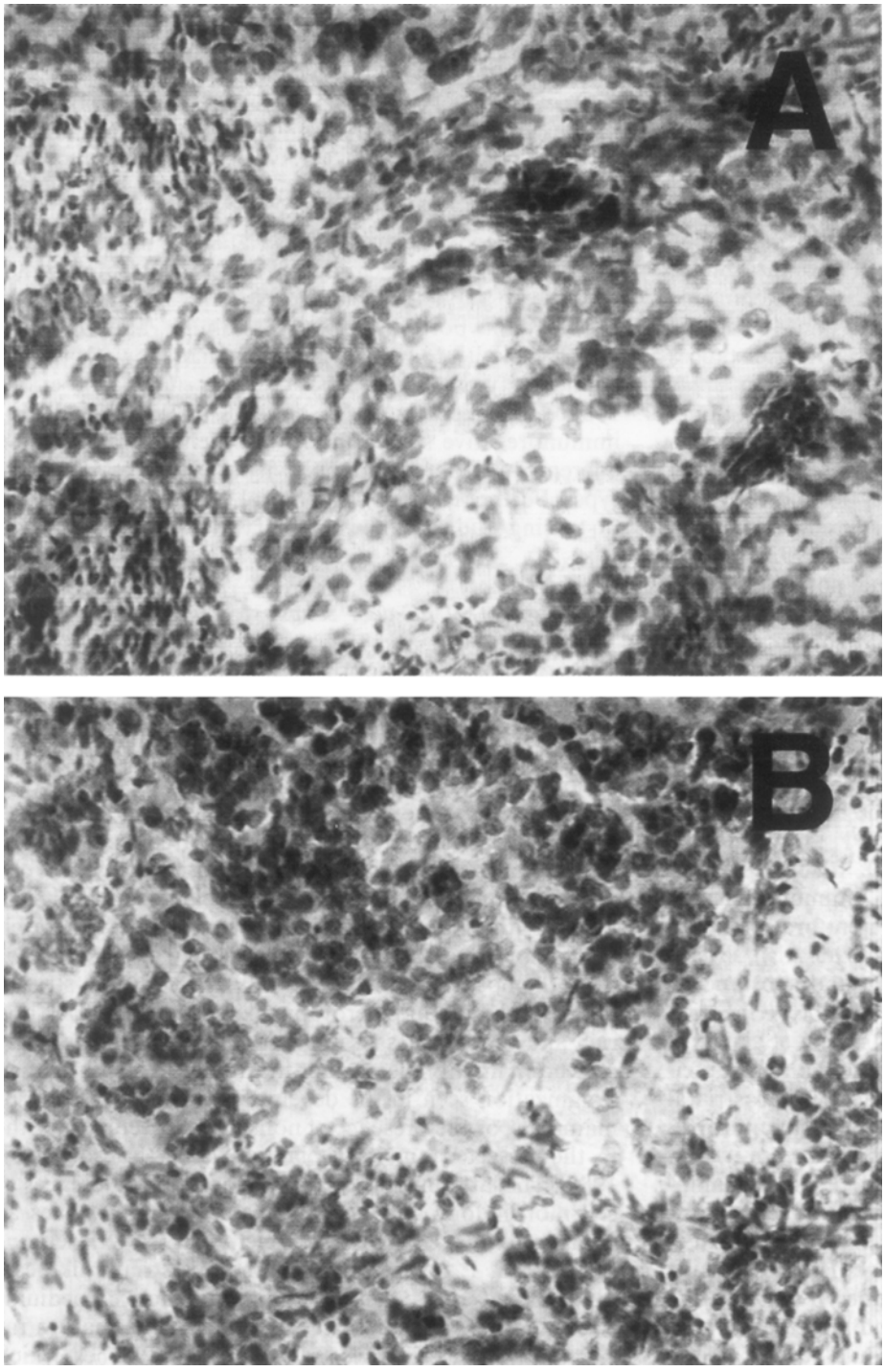

Fig. 5A,B. Close-up magnification of the regions within the white boxes in Fig. 4C and D, respectively. **A** Cresyl violet-stained cells within the lateral ganglionic eminence graft in Fig. 4C; **B** cresyl violet-stained cells within the medial ganglionic eminence graft in Fig. 4D

The following discussion explores each of these points separately.

The functional significance of the increased AChE-rich fraction in LGE grafts

Intrastriatal infusion of the excitatory amino acids produces a series of neuropathologic changes similar to those found in Huntington disease (Coyle and Schwarcz 1976; Hantraye et al. 1990; McGeer and McGeer 1976). In animal models, these changes are accompanied by certain locomotor and behavioral abnormalities that are ameliorated by subsequent intrastriatal engraftment of fetal striatal tissue in affected rats (Deckel et al. 1983, 1986; Dunnett et al. 1988; Isacson et al. 1984, 1986) and in affected nonhuman primates (Hantraye et al. 1992; Schumacher et al. 1992). This behavioral recovery is thought to be caused by establishment of structural and functional connections between the graft and the host

neurons (Björklund et al. 1987; Giordano et al. 1988; Isacson et al. 1984). Evidence for structural graft-host connectivity is provided by studies employing anterograde and retrograde tracers to demonstrate afferent connections between the graft and the host substantia nigra, cortex, thalamic intralaminar nuclei, and amygdala (Labandeira-Garcia et al. 1991; Wictorin and Björklund 1989; Wictorin et al. 1988, 1989a; Xu et al. 1989, 1991a), and efferent connections with the globus pallidus, entopeduncular nucleus, and substantia nigra (Wictorin et al. 1989c, 1990b). Furthermore, xenogenic transplantation experiments show that immunolabeled axons of the grafted neurons extend over long distances to innervate the appropriate striatal projection areas (Wictorin et al. 1990a, 1991). The evidence for direct functional graft-host interaction is provided by changes in neuropeptide messenger RNA (mRNA) expression and Fos protein induction in striatal grafts produced by manipulation of the host dopaminergic afferents (Campbell et al. 1992; Liu et al. 1991; Mandel et al. 1992), and by electrophysiologic recording of synaptic potentials in the graft neurons after cortical and thalamic electrical stimulation (Wilson et al. 1990; Xu et al. 1991b).

Importantly, much of this graft-host structural and functional connectivity seems to be limited to the the AChE-rich zones within the graft. Specifically, the AChE-rich zones closely correspond to zones immunoreactive for D_1 receptor-related phosphoprotein DARPP-32 and are selectively innervated by the host dopaminergic fibers (Labandeira-Garcia et al. 1991; Graybiel et al. 1989; Liu et al. 1990; Wictorin et al. 1988, 1989b). In addition, these AChE-rich, DARPP-32-immuno-reactive regions are the principal source of efferent projections to the host brain (Wictorin et al. 1989b, 1989c). Also, several striatal markers, including enkephalin and substance P immunoreactivity, exclusively localize to the AChE-rich zones (P zones; Graybiel et al. 1989; Isacson et al. 1987). Interference with the afferent dopaminergic control, either by 6-hydroxydopamine lesions of the nigrostriatal tract or by haloperidol treatment, produces an appropriate increase in preproenkephalin and a decrease in preprotachykinin mRNA expression in the P zones (Campbell et al. 1992). Dopaminergic agonists induce expression of Fos protein exclusively within the P zones (Liu et al. 1991; Mandel et al. 1992). Taken together, these results strongly suggest that AChE-rich zones constitute the part of the graft that is structurally and functionally connected to the host brain, and that it would be desirable to increase the proportion of AChE-rich zones in striatal grafts.

To date, the standard dissection of the striatum primordium for transplantation has included both the medial and the lateral ganglionic eminences of the basal telencephalon, as reviewed by Dunnett and Björklund (1992). However, previous studies do not provide quantitative data on the proportion of AChE-rich and -poor zones in the resultant grafts. In our own experience, transplanting the two ganglionic eminences jointly using this standard dissection, AChE-rich zones usually comprise about 20–40% of the graft (Isacson et al. 1987). This estimate is compatible with the apparent proportion of AChE-rich zones in photomicrographs of grafts published by other groups (Labandeira-Garcia et al. 1991; Liu et al. 1990; Walker et al. 1987; Wictorin et al. 1989b). In contrast, we show here that by limiting the dissection to the lateral ganglionic eminence, the average AChE-rich fraction is increased to 87%. Furthermore, we have demonstrated that it is possible to produce an entirely AChE-rich graft. Since a number of previous studies have shown that AChE-poor zones contain nonstriatal-like tissue (Difiglia et al. 1988; Graybiel et al. 1989) that lacks connections with the host (Wictorin et al. 1989b), and since graft zones that exhibit both dark AChE-staining and TH immunoreactivity coincide with zones that show reciprocal connectivity with the host circuitry (Wictorin et al. 1989b), it is likely that LGE-derived AChE-rich and TH-immunoreactive striatal grafts will demonstrate greater afferent and efferent connectivity than do mixed graft types. Further electrophysiological, biochemical, and axon tracing studies will be necessary to test this prediction.

The origin of AChE-poor zones

The origin of AChE-poor zones in fetal striatal grafts has been the subject of much debate. In agreement with previous reports (Graybiel et al. 1989; Isacson et al. 1987), we found a uniformly high density of Nissl-stained cells in both the AChE-rich and -poor zones of the grafts. This finding excludes the possibility that clustering of neurons is an explanation for the patchy AChE architecture of the grafts. Nor is the patchy architecture a result of incorporation of nongraft tissue, since prelabeling fetal graft cells with [^{3}H]thymidine demonstrates that both AChE-rich and -poor zones derive from the grafted tissue and not from the host (Graybiel et al. 1989). In addition, striatal grafts implanted in heterotopic loci also develop AChE-rich and -poor zones (Isacson et al. 1987). This graft architecture might reflect either the immature patch-matrix organization seen in the developing normal striatum of mammals, or the presence of nonstriatal precursors within the dissected and transplanted tissue (Isacson et al. 1987). The latter hypothesis is supported by differences in cell morphology and histochemistry within P zones as compared to NP zones. Graybiel et al. (1989) demonstrated that P zones contain numerous striatal-like calbindin- and met-enkephalin-immunoreactive medium-sized neurons, similar to those found in the mature rat striatum. These cell types are lacking in NP zones, which instead contain large multipolar aspiny calbindin-positive neurons that are not typically found in the normal striatum.

The possibility that AChE-poor zones in striatal grafts may arise from non-striatal tissue, or, more precisely, from fetal neuroblasts that are not committed to a striatal fate, raises the question of which nonstriatal precursors might be inadvertently included in the dissected and transplanted fetal tissue. The anlagen of globus pallidus, cortex, amygdala, and olfactory tubercle are found in close proximity to the telencephalic ganglionic eminences (Fentress et al. 1981; Smart and Sturrock 1979), and their unintended inclusion in the dissected donor

tissue could contaminate the striatal preparation. Furthermore, there is evidence that cells of the adult globus pallidus arise from both the fetal diencephalon and the telencephalic MGE (Marchand and Lajoie 1986; Nieuwenhuys 1977; Smart and Sturrock 1979). Dissections of striatum primordium that include the MGE may therefore incorporate a portion of the pallidal anlage. Since the mature globus pallidus is distinguished from adult neostriatal tissue by minimal TH immuno-reactivity and poor AChE staining, it is possible that these characteristics of the AChE-poor, TH-poor regions of grafts derive from cells committed to a pallidal fate at the time of transplantation. Further support of this hypothesis is provided by Difiglia et al. (1988), who find regions of neuropil within the striatal graft that have a synaptic and neuronal morphology reminiscent of globus pallidus.

The predominance of AChE-poor regions in our MGE grafts and the paucity of these regions in the LGE grafts suggest that the AChE-poor regions originate from cells within the MGE that are destined for a nonneostriatal (probably pallidal) fate and from cells of extraganglionic tissue contaminating the dissection . In addition, it is possible that there is more than one type of AChE-poor zone in the grafts. Specifically, the AChE-poor regions in LGE grafts could be of a different type than those found in MGE grafts, perhaps reflecting the patch-matrix organization of the normal immature striatum (Isacson et al. 1987). Given the limits of our dissection technique and the inclusion of a few AChE-rich zones in some of the MGE grafts and a few AChE-poor zones in some of the LGE grafts, it cannot be stated with absolute certainty that there is a complete correspondence between cell fate and location within one of the two ganglionic eminences. Nevertheless, this study demonstrates that by E14 in the rat the vast majority of LGE cells that will survive the transplantation procedure have already become committed to a morphotype that is AChE-positive and dopamine-receptive, as are normal striatal cells, whereas at most only a few percent of cells from the MGE will express these characteristics.

Effect of selective dissection of ganglionic eminences on graft size, morphology, and connectivity

One of the most striking findings of this study is the greater morphological integration of LGE grafts into the host striatum, when compared with MGE grafts or those derived from both ganglionic eminences. Intrastriatal grafts that include cells from outside of the LGE grow into the host striatum as a cohesive unit that excludes host tissues and displaces surrounding fiber tracts outward from the graft. In contrast, the almost exclusively AChE-rich grafts derived from LGE tissue appear to grow into the host striatum in an infiltrative fashion, such that graft tissue becomes interdigitated among penetrating fiber bundles. This effectively reconstitutes the characteristic morphological pattern for which the corpus striatum is named. The cohesiveness of intrastriatal grafts containing cells from non-LGE tissues may therefore be an artifact of heterotypic cell-cell interactions and not an inherent feature of fetal striatal transplants. The observation that MGE grafts also show a tendency toward smaller graft size may further reflect the consequences of heterotopic implantation of nonstriatal tissue into the host striatum. Homotopic grafts have been found to survive better and grow to a larger size than comparable heterotopic grafts, presumably because of site-specific trophic influences (Deckel et al. 1984, 1986; Isacson et al. 1987). A larger study with greater statistical power would be required to definitively assess the effect of selective dissection of the ganglionic eminences on graft size.

Previous studies have indicated that specific striatal afferent projections, such as from neocortex or thalamus, not only are physically displaced by graft growth, but also are only able to penetrate very short distances into the periphery of heterotypic grafts (Wictorin and Björklund 1989; Wictorin et al. 1988). The morphological interdigitation of the LGE grafts with the host may increase the opportunity for penetration of the graft core by afferent axons. Furthermore, heterotypic graft architecture may also be responsible for reduced efferent outgrowth of graft axons into the host. If the AChE-poor zones contain pallidal-like cells, as this study suggests, these may interfere with graft-host connectivity by competing with the host as proximal ectopic target zones for axons originating from neurons in the AChE-rich zones (Wictorin et al. 1991). Elimination of potentially competing target cells from within the graft may induce a larger portion of graft axons to seek more distant host targets. Further tracer, histochemical, and electrophysiological studies will determine whether AChE-rich LGE grafts enhance graft-host connectivity and behavioral recovery in animals receiving transplants.

Acknowledgements. This study was supported in part by PHS grants NS30064 and NS29178 to O. I.; P. P. was supported in part by NINDS training grant 5T32 NS07340; and T. D. was supported in part by a fellowship grant from the Department of Psychology, McLean Hospital. We would like to extend our thanks to John Park for excellent technical assistance.

References

Banker G, Goslin K (1991) Primary dissociated cell cultures of neural tissue. In: Banker G, Goslin K (eds) Culturing nerve cells. MIT, Cambridge, Mass., pp 41–71

Björklund A, Lindvall O, Isacson O, Brundin P, Wictorin K, Strecker RE, Clarke DJ, Dunnett SB (1987) Mechanisms of action of intracerebral neural implants: studies on nigral and striatal grafts to the lesioned striatum. Trends Neurosci 10:509–516

Brundin P, Isacson O, Björklund A (1985) Monitoring of cell viability of embryonic CNS tissue as a criterion for intracerebral graft survival. Brain Res 331:251–259

Campbell K, Wictorin K, Björklund A (1992) Differential regulation of neuropeptide mRNA expression in intrastriatal striatal transplants by host dopaminergic afferents. Proc Natl Acad Sci USA 89:10489–93

Coyle JT, Schwarcz R (1976) Lesion of striatal neurons with kainic acid provides a model for Huntington's chorea. Nature 263:244–246

Deckel AW, Robinson RG, Coyle JR, Sanberg PR (1983) Reversal of long-term locomotor abnormalities in the kainic acid model

of Huntington's disease by day 18 fetal striatal implants. Eur J Pharmacol 93:287–288
Deckel AW, Robinson RG, Newman DB (1984) Use of Golgi and Nissl stain to evaluate a chronic neurodegeneration of cortically transplanted fetal rat striatum. Soc Neurosci Abstr 10. 463
Deckel AW, Moran TH, Coyle JT, Sanberg PR, Robinson RG (1986) Anatomical predictors of behavioral recovery following fetal striatal transplants. Brain Res 365:249–258
Difiglia M, Schiff L, Deckel W (1988) Neuronal organization of fetal striatal grafts in kainate- and sham-lesioned rat caudate nucleus: light and electron-microscopic observations. J Neurosci 8:1112–1130
Dunnett SB, Björklund A (1992) Staging and dissection of rat embryos. In: Dunnett SB, Björklund A (eds) Neural transplantation: a practical approach. Oxford University Press, New York, pp 15–16
Dunnett SB, Isacson O, Sirinathsinghji DJS, Clarke DJ, Björklund A (1988) Striatal grafts in rats with unilateral neostriatal lesions: recovery from dopamine dependent motor assymetry and deficits in skilled paw-reaching. Neuroscience 24:813–820
Fentress JC, Stanfield BB, Cowan WM (1981) Observations on the development of the striatum in mice and rats. Anat Embryol 163:275–298
Giordano M, Hagenmeyer-Houser SH, Sanberg PR (1988) Intraparenchymal fetal striatal transplants and recovery in kainic acid lesioned rats. Brain Res 446:183–188
Graybiel AM, Liu FC, Dunnett SB (1989) Intrastriatal grafts derived from fetal striata primordia. I. phenotypy and modular organization. J Neurosci 9:3250–3271
Hantraye P, Riche D, Maziere M, Isacson O (1990) A primate model of Huntington's disease: behavioral and anatomical studies of unilateral excitotoxic lesions of the caudate-putamen in the baboon. Exp Neurol 108:91–104
Hantraye P, Riche D, Maziere M, Isacson O (1992) Intrastriatal transplantation of cross-species fetal striatal cells reduces abnormal movements in a primate model of Huntington disease. Proc Natl Acad Sci USA 89:4187–4191
Helmes GA, Palmer PE, Simmons NE, DiPierro C, Bennett JP (1992) Descriptive morphology of developing fetal neostriatal allografts in the rhesus monkey: a correlated light and electron microscopic golgi study. Neuroscience 50:163–179
Isacson O, Brundin P, Kelly PAT, Gage FH, Björklund A (1984) Functional neuronal replacement by grafted striatal neurons in the ibotenic-acid lesioned rat striatum. Nature 311:458–460
Isacson O, Dunnett SB, Björklund A (1986) Graft-induced behavioral recovery in an animal model of Huntington disease. Proc Natl Acad Sci USA 83:2728–2732
Isacson O, Dawbarn D, Brundin P, Gage FH, Emson PC, Björklund A (1987) Neural grafting in a rat model of Huntington's disease: striosomal-like organization of striatal grafts as revealed by acetylcholinesterase histochemistry, immunocytochemistry and receptor autoradiography. Neuroscience 22:481–497
Koelle GB (1954) The histochemical localization of cholinesterases in the central nervous system of the rat. J Comp Neurol 100:211–235
Labandeira-Garcia JL, Wictorin K, Cunningham ET, Björklund A (1991) Development of intrastriatal striatal grafts and their afferent innervation from the host. Neuroscience 42:407–426
Liu FC, Graybiel AM, Dunnett SB, Baughman RW (1990) Intrastriatal grafts derived from fetal striatal primordia. II. Reconstitution of cholinergic and dopaminergic systems. J Comp Neurol 295:1–14
Liu FC, Dunnett SB, Robertson HA, Graybiel AM (1991) Intrastriatal grafts derived from fetal striata primordia. III. Induction of modular patterns of Fos-like immunoreactivity by cocaine. Exp Brain Res 85:501–506
Mandel RJ, Wictorin K, Cenci MA, Björklund A (1992) Fos expression in intrastriatal striatal grafts: regulation by host dopaminergic afferents. Brain Res 583:207–215
Marchand R, Lajoie L (1986) Histogenesis of the striopallidal system in the rat: neurogenesis of its neurons. Neuroscience 17:573–590
McGeer EG, McGeer PL (1976) Duplication of biochemical changes in Huntington's chorea by intrastriatal injection of glutamic and kainic acids. Nature 263:517–519
Nieuwenhuys R (1977) Aspects of the morphology of the striatum. In: Cools AR, Lohman AHM, Van Den Bercken JHL (eds) Psychobiology of the striatum. Elsevier, Amsterdam, pp 1–19
Schumacher JM, Hantraye P, Brownell AL, Riche D, Madras B, Davenport PD, Maziere M, Elmaleh DR, Brownell GL, Isacson O (1992) A primate model of Huntington's disease: functional neural transplantation and CT-guided stereotactic procedures. Cell Transplantation 1:313–322
Smart IHM, Sturrock RR (1979) Ontogeny of the neostriatum. In: Divac I, Öberg RGE (eds) The neostriatum. Pergamon, Oxford, pp 127–146
Walker P, Chovanes GI, McAllister JP (1987) Identification of acetylcholinestrase-reactive neurons and neuropil in neostriatal transplants. J Comp Neurol 259:1–12
Wictorin K, Björklund A (1989) Connectivity of striatal grafts implanted into the ibotenic acid-lesioned striatum. II. Cortical afferents. Neuroscience 30:297–311
Wictorin K, Isacson O, Fischer W, Nothias F, Peschanski M, Björklund A (1988) Connectivity of striatal grafts implanted into the ibotenic acid-lesioned striatum. I. Subcortical afferents. Neuroscience 27:547–562
Wictorin K, Clarke DJ, Bolam JP, Björklund A (1989a) Host corticostriatal fibers establish synaptic connections with grafted striatal neurons in the ibotenic acid-lesioned striatum. Eur J Neurosci 1:189–195
Wictorin K, Ouimet CC, Björklund A (1989b) Intrinsic organization and connectivity of intrastriatal striatal transplants in rats as revealed by DARPP-32 immunohistochemistry. Eur J Neurosci 1:690–701
Wictorin K, Simerly RB, Isacson O, Swanson LW, Björklund A (1989c) Connectivity of striatal grafts implanted into the ibotenic acid-lesioned striatum. III. Efferent projecting graft neurons and their relation to host afferents within graft. Neuroscience 30:313–330
Wictorin K, Brundin P, Gustavii B, Lindvall O, Björklund A (1990a) Reformation of long axon pathways in adult rat CNS by human forebrain neuroblasts. Nature 347:556–558
Wictorin K, Clarke DJ, Bolam JP, Björklund A (1990b) Fetal striatal neurons grafted into the ibotenate-lesioned adult striatum: efferent projections and synaptic contacts in the host globus pallidus. Neuroscience 37:301–315
Wictorin K, Lagenaur CF, Lund RD, Björklund A (1991) Efferent projections to the host brain from intrastriatal striatal mouse to rat grafts: time course and tissue-type specificity as revealed by a mouse specific neuronal marker. Eur J Neurosci 3:86–101
Wilson CJ, Xu ZC, Emson PC, Feler C (1990) Anatomical and physiological properties of the cortical and thalamic innervations of neostriatal tissue grafts. Prog Brain Res 82:417–426
Xu ZC, Wilson CJ, Emson PC (1989) Restoration of the corticostriatal projection in rat neostriatal grafts: electron microscopic analysis. Neuroscience 29:539–550
Xu ZC, Wilson CJ, Emson PC (1991a) Restoration of thalamostriatal projections in rat neostriatal grafts: an electron microscopic analysis. J Comp Neurol 303:22–34
Xu ZC, Wilson CJ, Emson PC (1991b) Synaptic potentials evoked in spiny neurons in rat neostriatal grafts by cortical and thalamic stimulation. J Neurophysiol 65:477–493